



HAL
open science

Pectin methylesterification modulates cell wall properties to promote neighbour proximity-induced hypocotyl growth

Fabien Sénéchal

► **To cite this version:**

Fabien Sénéchal. Pectin methylesterification modulates cell wall properties to promote neighbour proximity-induced hypocotyl growth. 2023. hal-04461425

HAL Id: hal-04461425

<https://hal.science/hal-04461425>

Preprint submitted on 16 Feb 2024

HAL is a multi-disciplinary open access archive for the deposit and dissemination of scientific research documents, whether they are published or not. The documents may come from teaching and research institutions in France or abroad, or from public or private research centers.

L'archive ouverte pluridisciplinaire **HAL**, est destinée au dépôt et à la diffusion de documents scientifiques de niveau recherche, publiés ou non, émanant des établissements d'enseignement et de recherche français ou étrangers, des laboratoires publics ou privés.

1 **RESEARCH REPORT**

2

3 **Running title:** Cell wall modulates shade-induced hypocotyl growth

4

5 **Corresponding author**

6 Fabien S en echal, UMR INRAE 1158 BioEcoAgro, Plant Biology and Innovation, University
7 of Picardie Jules Verne, Amiens, France.

8 **Article title**

9 Pectin methylesterification modulates cell wall properties to promote neighbour proximity-
10 induced hypocotyl growth

11

12 **Authors**

13 Fabien Sénéchal¹, Sarah Robinson², Evert Van Schaik³, Martine Trévisan¹, Prashant Saxena¹,
14 Didier Reinhardt³, Christian Fankhauser¹

15

16 ¹: Centre for Integrative Genomics, Faculty of Biology and Medicine, Génopode Building,
17 University of Lausanne, Lausanne, Switzerland.

18 ²: Institute of Plant Sciences, University of Bern, Bern, Switzerland.

19 ³: Department of Biology, University of Fribourg, Fribourg, Switzerland.

20 **One sentence summary**

21 The degree of methylesterification of pectins modulates global changes in the cell wall and its
22 mechanical properties that contribute to the neighbour proximity-induced hypocotyl growth in
23 Arabidopsis

24 **Footnotes**

25 **Author's contribution**

26 **Conceptualization:** CF, DR, FS, SR, EVS. **Formal analysis:** FS, SR, EVS, MT, PS.
27 **Funding acquisition:** CF, DR. **Investigation:** FS, SR, EVS, MT, PS. **Project**
28 **administration:** CF, DR. **Software:** PS, SR, FS, EVS. **Validation:** FS, SR, EVS, CF, DR.
29 **Visualization:** FS, SR, EVS. **Supervision:** CF, DR. **Writing – Original Draft Preparation:**
30 FS, SR, EVS. **Writing – Review & Editing:** FS, SR, DR, CF

31

32 **Funding information**

33 This work was supported by grant “Plant Growth 2 in a Changing Environment” funded by
34 the Swiss initiative in systems biology (SystemX.ch) to Cris Kuhlemeier (Bern), Didier
35 Reinhardt (Fribourg) and Christian Fankhauser (Lausanne). Work in the Fankhauser lab was
36 supported by the University of Lausanne.

37

38 **Present address**

39 Fabien Sénéchal: UMR INRAE 1158 BioEcoAgro, Plant Biology and Innovation, University
40 of Picardie Jules Verne, Amiens, France.

41 Sarah Robinson: The Sainsbury Laboratory, University of Cambridge, Bateman Street
42 Cambridge, United Kingdom

43 Evert Van Schaik : University of Applied Sciences Leiden, Leiden, Netherlands

44 Prashant Saxena: James Watt School of Engineering, University of Glasgow, Glasgow,
45 United Kingdom

46

47 **Corresponding author email**

48 fabien.senechal@u-picardie.fr

49

50 **Abstract**

51 Plants growing with neighbours compete for light and consequently increase growth of their
52 vegetative organs to enhance access to sunlight. This response, called shade avoidance
53 syndrome (SAS), involves photoreceptors such as phytochromes as well as phytochrome
54 interacting factors (PIFs), which regulate the expression of growth-mediating genes.
55 Numerous cell wall-related genes belong to the putative targets of PIFs, and the importance of
56 cell wall modifications for enabling growth was extensively shown in developmental models
57 such as dark-grown hypocotyl. However, the role of the cell wall in the growth of de-
58 etiolated seedlings regulated by shade cues remains poorly established. Through analyses of
59 mechanical and biochemical properties of the cell wall coupled with transcriptomic analysis
60 of cell wall-related genes, we show the importance of cell wall modifications in neighbour
61 proximity-induced elongation. Further analysis using loss-of-function mutants impaired in the
62 synthesis and remodeling of the main cell wall polymers corroborated this. We focused on the
63 *cgr2cgr3* double mutant that is defective in homogalacturonan (HG) methyltransferase
64 activity required for methylesterification of HG-type pectins. By following hypocotyl growth
65 kinetically and spatially and analyzing the mechanical and biochemical properties of cell
66 walls, we found that methylesterification of HG-type pectins was required to enable global
67 cell wall modifications. Moreover, HG-class pectin modification was needed for plant
68 competition-induced hypocotyl growth. Collectively our work suggests that in the hypocotyl
69 PIFs orchestrate changes in the expression of numerous cell wall genes to enable neighbour
70 proximity-induced growth.

71 **Introduction**

72 Plants growing in dense populations compete for light required for photosynthesis
73 (Fiorucci and Fankhauser, 2017). Proximity of competitors and shade are perceived as a
74 change in light intensity and quality, resulting in various developmental adaptations (Galvão
75 and Fankhauser, 2015). Depending on their response to shade, plants are classified into shade-
76 tolerant and shade-avoiding species (Gommers et al., 2013). The latter react to shade with
77 characteristic growth responses in order to reach full sunlight for photosynthesis. This
78 phenomenon, known as Shade-Avoidance Syndrome (SAS) can be observed in most aerial
79 organs and involves a range of developmental changes (Pierik and De Wit, 2014). For
80 example, SAS entails early flowering and inhibition of branching, leaves adopt an upright
81 position (hyponasty), and petioles, stems and hypocotyls elongate (de Wit et al., 2016). These
82 changes accelerate the life cycle of plants and warrant survival and propagation under limited
83 light availability.

84 The phytochrome (phy) type photoreceptors have a central role in SAS with phyB
85 playing a predominant role in *Arabidopsis thaliana* (Legris et al., 2019). Under high R:FR
86 conditions, corresponding to full sunlight, active phyB moves into the nucleus, where it
87 interacts with transcription factors known as Phytochrome Interacting Factors (PIFs) to inhibit
88 their activities. Low R:FR conditions, on the other hand, cause inactivation of phyB and
89 derepression of the PIFs, which modulate genes required for shade-induced growth (de Wit et
90 al., 2016). A central mechanism in shade-induced growth is auxin biosynthesis in cotyledons
91 and young leaves followed by polar transport and distribution in hypocotyls and stems, which
92 elongate in response to shade (de Wit et al., 2014). phyB and PIFs also act locally in the
93 hypocotyl to promote growth through mechanisms that are less clearly established (Fiorucci
94 and Fankhauser, 2017; Pucciariello et al., 2018). For example PIFs regulate the expression of
95 genes required for plasma-membrane lipid biogenesis in the hypocotyl (Ince et al., 2022).
96 Moreover, numerous genes encoding cell wall-modifying proteins are induced by shade and
97 targeted by PIFs (Kohnen et al., 2016; Pedmale et al., 2016), suggesting role for cell wall
98 metabolism in the establishment of the shade-regulated growth.

99 The primary cell wall of growing plant organs has seemingly contradictory functions.
100 On the one hand, it provides mechanical strength to maintain cell shape and plant stature, on
101 the other hand, it has to remain elastic and plastic to allow cell expansion and plant growth
102 (Bashline et al., 2014). In dicotyledonous species such as *Arabidopsis*, the primary cell wall
103 consists of interconnected networks of polysaccharides and structural proteins/glycoproteins
104 (Cosgrove, 2005; Wolf et al., 2012a; Nguema-Ona et al., 2014). A first network of cellulose
105 microfibrils cross-linked by hemicelluloses (network 1) is embedded in a second network
106 made by pectins that have gelling properties (network 2). Pectins are intimately associated
107 with a third network (network 3), consisting mainly of glycoproteins such as extensins
108 (EXTs) and arabinogalactan proteins (AGPs) (Hijazi et al., 2014). This complex three-
109 dimensional mesh resists to internal turgor pressure, and at the same time yields to allow cell
110 growth. Dynamic adjustment of physical cell wall properties (e.g. stiffness, elasticity,
111 plasticity) involves cell wall-synthesizing and modifying enzymes that usually belong to

112 multigenic families and constantly modulate cell walls to allow growth (Atmodjo et al., 2013;
113 Sénéchal et al., 2014b; Pauly and Keegstra, 2016; Showalter and Basu, 2016).

114 Cell wall remodeling plays a central role in the control of seedling development,
115 however, its contribution to adaptive growth phenomena in response to environmental cues
116 such as SAS remains poorly understood. Although transcriptomic analyses suggested that cell
117 wall remodeling may play a central role in adaptive growth processes (Kohnen et al., 2016),
118 direct functional evidence is scarce. A role for xyloglucans in SAS has been established for
119 petiole elongation in *Arabidopsis* (Sasidharan et al., 2010; Sasidharan and Pierik, 2010), and
120 for shade-induced growth in *Stellaria longipes* (Sasidharan et al., 2008). Here, we took a
121 systematic approach to explore the contribution of cell wall remodeling in SAS of the
122 *Arabidopsis* hypocotyl. By combining Fourier-transformed infrared (FTIR) analyses of cell
123 wall constituents with measurements of cell wall biophysics, we show that cell wall
124 remodeling is triggered at early stages of the growth response induced by low R:FR,
125 indicative of neighbour proximity that is a form of SAS. Employing systematic transcriptomic
126 and genetic analysis with mutants affected in various aspects of cell wall biosynthesis and
127 modification, we establish pectin methylesterification status as a central determinant of cell
128 wall extensibility in the neighbour proximity-induced hypocotyl growth.

129

130 **Results**

131 **Low R:FR induces cell elongation mainly in the middle part of the hypocotyl**

132 In order to simulate the proximity of competing neighbours, we subjected Arabidopsis
133 seedlings to white light supplemented with far red (low R:FR ratio). Within one day, this led
134 to increased hypocotyl growth compared to control seedlings kept in white light (high R:FR
135 ratio) (**Fig. 1A**). In order to determine the site of growth, we used the borders of epidermal
136 cells as marks, since hypocotyl elongation proceeds almost exclusively by cell elongation
137 without cell division. In order to assess cell dimensions, confocal images of seedlings were
138 segmented in MorphoGraphX (de Reuille et al., 2015), followed by semiautomated cell size
139 measurements. Cell length along the length of the hypocotyl was increased by low R:FR
140 primarily in the middle part of the hypocotyl (**Fig. 1B**).

141

142 **Low R:FR changes mechanical properties of hypocotyl cell walls**

143 To assess the mechanical properties of the hypocotyl during growth induced by low
144 R:FR, we used an automated confocal micro-extensometer (Robinson et al., 2017). This
145 approach enabled *in vivo* quantification of the elastic properties of cell walls. Hypocotyls of
146 intact seedlings were abraded by freezing and thawing and subjected to repeated cycles of
147 application and removal of 5 mN of force. Our analysis revealed increased strain under low
148 R:FR after one day of treatment, and decreased strain after three days (**Fig. 2A**). Interestingly
149 this effect was specific to low R:FR conditions, since no such changes were observed under
150 high R:FR (**Fig. 2A**).

151 To relate growth and mechanical changes induced by low R:FR to cell wall properties,
152 we applied Fourier-transformed infrared (FTIR) microspectroscopy to cells located in the
153 middle part of the hypocotyl. The relative absorbance intensities for wavelengths related to
154 the cell wall (from 830 to 1800 cm^{-1}) were selected to assess the composition and status of
155 various cell wall polysaccharides. FTIR analysis revealed significantly different patterns of
156 relative absorption induced by low R:FR ratio after three days of treatment (**Fig. 2B and Fig.**
157 **S1**). The main differences were observed between 1530 and 1200 cm^{-1} and between 1180 and
158 1030 cm^{-1} (**Fig. 2B**). A relative decrease (at 1740 and between 1530-1200 cm^{-1}) indicates
159 lower levels of pectins and xyloglucans, as well as cellulose and lignin. On the other hand, an
160 increase between 1180 and 1030 cm^{-1} indicates enrichment of pectins, xyloglucans, cellulose
161 and arabinogalactan that can relate both to AGPs and rhamnogalacturonan I-type pectins (**Fig.**
162 **2B**). These results indicate major cell wall remodeling in response to low R:FR ratio. In order
163 to obtain further insight into the changed cell wall components, we performed hierarchical
164 clustering for the wavelengths that have previously been assigned to certain cell wall
165 components (Kakuráková et al., 2000; Wilson et al., 2000; Mouille et al., 2003; Alonso-simón
166 et al., 2011; Szymanska-Chargot and Zdunek, 2013; Largo-Gosens et al., 2014) (**Fig. 2C**).
167 This revealed an overall enrichment for pectins with a low degree of methylesterification (de-
168 esterified pectins), in addition to other pectins, arabinogalactan proteins, cellulose, and
169 xyloglucans in response to low R:FR, while other wavelengths assigned to pectins, cellulose

170 and xyloglucans showed opposite trends. Depending on the chemical bonds revealed by the
171 wavelengths, different structural part of the polysaccharides are assessed such as backbone
172 and side chains. This could explain opposite trends for wavelengths related to the same
173 polysaccharide, which can be more abundant with reduced side chains for instance. Taken
174 together, these results revealed major changes in cell wall biosynthesis and remodeling in
175 response to low R:FR.

176

177 **Low R:FR impinges on expression of cell wall-related genes**

178 In order to investigate transcriptional regulation of cell wall properties under low
179 R:FR, we considered 40 gene families that are thought to be involved in synthesis and/or
180 remodeling of cell wall components. The expression of a total of 824 genes was analyzed
181 using an RNA sequencing dataset from a time course experiment under low R:FR conditions
182 (Kohnen et al., 2016). In this set of genes, 544 were found to be expressed in seedlings grown
183 under control conditions, among which 224 were regulated by low R:FR in hypocotyls (**Fig.**
184 **3A**). Only few genes were regulated in cotyledons or in both organs (26 and 16 genes,
185 respectively) (**Fig. 3A**). Most genes were regulated at later stages (90 or 180 min after onset
186 of light stimulus), and they were mostly up-regulated, in particular in hypocotyls (**Fig. 3A**).
187 Modulated genes comprised functions related to (hemi)cellulose (network 1), pectin (network
188 2), and structural proteins (network 3) (**Fig. 3B**). The few genes that were induced at the early
189 time points (15 or 45 min. after onset of the light stimulus) in hypocotyls are involved in cell
190 wall remodelling (At1g49490:EXT, At5g47500:PME, At1g62760:PMEI, At5g02260:EXP,
191 At5g57560:XTH, At1g02405:EXT, At3g10710:PME, **Tables S1A and S1B**). Considering the
192 global influence of FR light on cell biosynthetic genes, the highest percentage related to
193 pectins (network 2) with 96% of the genes expressed in seedlings, and 52% affected by low
194 R:FR conditions. Taken together, these results indicate that cell wall remodelling is initiated
195 within the first 15 minutes of low R:FR treatment, followed by general cell wall modifications
196 involving both synthesis and remodeling of all cell wall constituents, in particular of pectin.

197 SAS is controlled by PIFs, hence, we interrogated previously published ChIP
198 sequencing data (Kohnen et al., 2016) for interactions of PIF4 and PIF5 with the 224 genes
199 regulated in the hypocotyl under low R:FR conditions. Indeed, 59 genes showed a direct
200 interaction with PIF4 and/or PIF5 (**Fig. S2 and Table S1C**), including genes related to all
201 three polymer networks, as well as to all processes including cell wall synthesis, remodelling,
202 and signalling.

203

204 **Cell wall-related mutants reveal the role of cell wall components in low R:FR-induced** 205 **growth**

206 In order to gain insight into the mechanisms involved in low R:FR-induced growth,
207 loss-of-function mutants defective in the three networks (cellulose, pectin, glycoproteins)
208 were investigated for growth phenotypes under low R:FR treatment. We selected *xxt* mutants

209 impaired in xyloglucan biosynthesis (network 1), mutants affected in pectin biosynthesis
210 (*gaut*, *gat1* and *cgr*) and pectin remodeling (*pme* and *pmei*; network 2), and mutants affected
211 in AGP biosynthesis (*galt*, *agp10c*, and *fla9*; network 3). All of these mutants were subjected
212 to low R:FR treatment for three days and their hypocotyl growth response was normalized to
213 the wild type. None of the single mutants in network 1 had a growth phenotype (**Fig. 4A**),
214 possibly because of genetic redundancy, but the double mutants *txt1txt2* and *txt2txt5* showed
215 significantly reduced hypocotyl elongation in response to low R:FR. In network 2 mutants,
216 only *cgr2*, had a growth defect, which was exacerbated in the *cgr2cgr3* double mutant.
217 Unexpectedly, mutants affected in network 3 generally grew longer than the wild type (**Fig.**
218 **4A**). Taken together, these results highlight the importance of xyloglucan and pectin in SAS,
219 while some proteinaceous component of the cell walls appear to restricts hypocotyl elongation
220 in the wild type.

221 Based on the induction of several homogalacturonan methyltransferases (*HGMT*),
222 including the previously characterized *HGMT* genes *CGR2* and *CGR3* (Kim et al., 2015)
223 (**Fig. S3**), and on the strong growth phenotype of the *cgr2cgr3* double mutant, (**Fig. 4A**), we
224 investigated cell wall constituents in *cgr2cgr3* by FTIR analyses using wavelengths assigned
225 to methylesterified (1740 cm^{-1}) and demethylesterified (1630 cm^{-1}) pectins (**Fig. S4**). Using
226 these wavelengths we estimated the degree of methylesterification (DM), which was
227 decreased by approximately 40% in *cgr2cgr3* compared to the wild type. In a time course
228 experiment, *cgr2cgr3* was not affected in hypocotyl growth under control conditions (high
229 R:FR), however, under low R:FR conditions, growth was reduced (**Fig. 4B**). Notably,
230 *cgr2cgr3* reacted slower (4d+1d) and weaker (4d+3d) than the wild type (**Fig. 4B**). The
231 growth defect of *cgr2cgr3* was particularly pronounced in the middle part of the hypocotyl
232 that normally shows the strongest growth response (**Fig. S5**). This indicates that *cgr2cgr3*
233 mutants have a defect in low R:FR-induced epidermal cell elongation.

234 We next assessed the mechanical properties of *cgr2cgr3* hypocotyls in response to low
235 R:FR (**Fig. 4C**). Wild type hypocotyls had shown an increase in cell wall strain after 1d, and a
236 decrease after 3d of FR treatment (**Fig. 2A**). In contrast, *cgr2cgr3* did not show a change in
237 strain at either time point, indicating that cell wall remodeling is defective in the double
238 mutant. To further address this aspect, we investigated cell wall composition of *cgr2cgr3* by
239 FTIR microspectroscopy as in the wild type (**Fig. 2B,C**), in the range of wavelengths from
240 830 to 1800 cm^{-1} to obtain a cell wall fingerprint. This analysis was performed in the middle
241 part of hypocotyls which shows the strongest growth increment under low R:FR (**Fig. 1B**,
242 **Fig. S6**). Relative absorbances for Col-0 and *cgr2cgr3* did not show significant changes in
243 response to low R:FR after the first day (**Fig. 5A**; **Figs. S6A,B upper panels**). However, 3
244 days after transfer, both wild type and *cgr2cgr3* showed significant changes of relative
245 absorbances in response to low R:FR conditions (**Fig. 5A**; **Figs. S6A,B, lower panels**).
246 Overall, the pattern of the significantly affected wavelengths were similar for both genotypes,
247 but the differences were more pronounced in the wild type than *cgr2cgr3* (**Fig. 5B**).

248 The main differences between the genotypes were observed in the range of
249 wavelengths from 1630 to 1500 cm^{-1} with a decrease in the wild type but not in *cgr2cgr3*
250 (**Fig. 5B**), and between 1180 to 1030 cm^{-1} , where the wild type showed a stronger increase

251 than the double mutant. These results suggest that a change in pectin methylesterification in
252 *cgr2cgr3* results in secondary changes in cell wall composition (**Fig. 5B**).

253 Discussion

254 While growth is simple to quantify, in particular in an organ like the hypocotyl that
255 grows essentially in only one dimension, the underlying molecular mechanisms are extremely
256 complex because they involve multiple regulatory levels such as hormonal and metabolic
257 regulation, transcriptional activation of growth-related genes, and ultimately remodeling of
258 the complex three-dimensional cell wall polymer network. Thanks to the ease of mutational
259 analysis of growth, many of the upstream regulatory components in SAS have been identified
260 (Procko et al., 2014; Ballaré and Pierik, 2017; Fiorucci and Fankhauser, 2017). A reduced
261 R:FR indicative of neighbour proximity is primarily perceived by phyB in cotyledons and
262 young leaves (Ballaré and Pierik, 2017; Fiorucci and Fankhauser, 2017). This leads to PIF-
263 mediated induction of auxin production, which following transport to the hypocotyl promotes
264 elongation (Procko et al., 2014; Ballaré and Pierik, 2017; Fiorucci and Fankhauser, 2017).
265 PIFs can also directly regulate expression of hypocotyl specific genes as shown for genes
266 encoding enzymes involved in plasma-membrane biogenesis (Ince et al., 2022). Our data
267 suggests low R:FR induces extensive hypocotyl-specific regulation of genes encoding
268 enzymes involved in cell wall biosynthesis and remodeling (**Fig. 3**), that ultimately results in
269 in alteration of cell wall properties and induction of growth. However, due to the
270 interdependency of cell wall components, it has been difficult to disentangle the role of
271 individual cell wall components in growth. Here, we identified and characterized pectin
272 methylesterification status as a central element in the growth phenomenon of Arabidopsis
273 seedlings in the shade avoidance response.

274 Pectin consists mainly of homogalacturonan (HG) which represents a linear polymer
275 of galacturonic acid (GalA) synthesized by galacturonosyltransferases (GAUTs) and GAUT-
276 like (GATL) enzymes in the Golgi apparatus (Atmodjo et al., 2013). HG is subsequently
277 methylesterified by HGMTs before secretion into the cell wall, where it can be selectively
278 demethylesterified by pectin methylesterases (PMEs) (Sénéchal et al., 2014b). Thus, PME
279 activity adjusts the degree of methylesterification (DM), which in turn modulates cell wall
280 mechanical properties (Peaucelle et al., 2011; Wang et al., 2020). Furthermore, PME-
281 mediated demethylesterification can expose HG to pectin-degrading enzymes such as
282 polygalacturonases (PGs) and pectate lyases-like (PLLs) (Sénéchal et al., 2014b). Pectin
283 degradation by these enzymes can contribute to cell wall loosening. There is evidence for a
284 functional role of pectin metabolism in the regulation of growth (Bouton, 2002; Mouille et al.,
285 2007) (Pelletier et al., 2010; Guénin et al., 2011; Wolf et al., 2012b; Sénéchal et al., 2014a)
286 (Wang et al., 2010; Xiao et al., 2014; Rui et al., 2017), however, the high degree of
287 redundancy in cell-wall remodeling enzymes has complicated the analysis. For example, there
288 are 66 and 76 genes, respectively, that encode PMEs and PME inhibitors (PMEIs), allowing
289 for extensive compensatory responses upon genetic or pharmacological interference.

290 A mechanistic understanding of growth phenomena requires the combined use of
291 genetic, analytic, and biomechanical methods to identify the causal elements in cell growth.
292 Using FTIR analysis, we document changes in cell wall composition in response to changes in
293 the R:FR ratio, which correlate with accelerated growth. We identified two
294 homogalacturonan-methyltransferase (HGMT) genes (*CGR2* and *CGR3*) that are required for

295 neighbour proximity-induced growth. Biomechanical assays showed that *CGR2* and *CGR3*
296 contribute to cell wall extensibility at the onset of growth. Previous studies used atomic force
297 microscopy to analyze cell walls, which measures properties perpendicular to the direction
298 of growth, to detect differences in mechanical properties in plants with modified pectin that
299 correlated with growth (Peaucelle et al., 2008; Peaucelle et al., 2011; Braybrook and
300 Peaucelle, 2013; Peaucelle et al., 2015). In this study we were able to measure differences in
301 mechanical properties using an extensometer which measures properties in the direction of
302 growth. Both approaches show a correlation between modifying pectin chemistry, changes in
303 cell wall mechanical properties and growth, supporting a role of pectin in growth regulation.
304 Further work is required to understand the nature of this regulation and how it relates to the
305 other cell wall components (Coen and Cosgrove, 2023).
306

307 **Materials and Methods**

308 Information on the biological material and methods is available in the supplemental data

309 **Acknowledgement**

310 The authors wish to gratefully thank Prof. Kenneth Keegstra, Prof. Debra Mohnen, Prof.
311 Frederica Brandizzi and Prof. Jérôme Pelloux respectively for sharing seeds of the *xxt*, *gaut*,
312 *cgr* and *pme/pmei* mutants used in this study. We also thank Dr. Christiane Nawrath, Dr.
313 Sylvester Mazurek and Dr. Gregory Mouille for their help in the analysis of the FTIR
314 microspectroscopy. We thank the Swiss initiative in systems biology (SystemX.ch) and the
315 University of Lausanne for the funding support. We nicely thank Prof. Cris Kuhlemeier for
316 contributing to the funding acquisition and the co-supervising of the “Plant Growth 2 in a
317 Changing Environment” project funded by the Swiss initiative in systems biology
318 (SystemX.ch). We also thank him for his help in the project handing and for hosting Sarah
319 Robinson, postdoc in his lab during the project.

320

321 **Figure legends**

322 **Figure 1. Low R:FR induces fast growth in the middle part of the hypocotyl. (A)** Length
323 of the hypocotyls in response to high and low R:FR treatments. Col-0 seedlings were grown
324 for 4 days in high R:FR before being transferred under low R:FR (blue bars) or kept in high
325 R:FR (yellow bars) for 3 additional days. The bars show means in mm \pm confidence intervals
326 measured at 4 (4d), 5 (4d+1d) and 7 (4d+3d) days. Significant differences (indicated with
327 letters) were determined according to one-way Anova followed by a multiple comparisons
328 with Tukey's test. **(B)** Length of the hypocotyl epidermis cells in response to high and low
329 R:FR treatments. After 4 days under high R:FR (blue curve), Col-0 seedlings were grown for
330 1 day under high R:FR (red curve) or low R:FR (green curve). The length of the epidermis
331 cells were plotted from the top to the bottom part of the hypocotyl. The curves show means in
332 $\mu\text{m} \pm$ confidence intervals (shaded areas).

333 **Figure 2. Low R:FR induces changes in mechanical and cell wall properties of the**
334 **hypocotyl. (A)** Elastic properties of hypocotyl assessed under high and low R:FR treatment.
335 Hypocotyls were frozen and thawed then subjected to cycles of application and removal of 5
336 mN of force using an automated confocal micro extensometer (see methods). The average
337 magnitude of strain incurred by seedlings grown in a high R:FR (yellow bars) or low R:FR
338 (blue bars) light regime after 1 (4d+1d) and 3 days (4d+3d) is shown. Bright-field images
339 were collected every 645 ms and strain was computed from regions that were tracked in the
340 images using the ACME tracker software. The bars show means in % \pm SD ($n > 10$
341 independent seedlings, at least five oscillations were made). Pairwise comparisons were made
342 using Welch t-test brackets indicated statistical tests that were made with significance $p < 0.1^*$,
343 $p < 0.05^{**}$ and $p < 0.01^{***}$. **(B,C)** Cell wall properties in the middle part of the hypocotyl under
344 high and low R:FR treatments. Cell wall chemical bounds were analyzed by Fourier-
345 Transformed InfraRed (FTIR) microspectroscopy. For each hypocotyl, 6 spectra were
346 collected in the middle part, avoiding the central cylinder, for at least 5 independent
347 hypocotyls per condition. Baseline correction and data normalization were made for the
348 absorbances between 1810 and 830 cm^{-1} (corresponding to the cell wall fingerprint, see
349 **Supplemental Figure S1**). Pairwise comparison between high and low R:FR was made after
350 1 and 3 days treatments and significant differences were identified using Student's t-test for
351 each wavelength. **(B)** All Student's t-values were plotted against wavelengths with horizontal
352 lines referring to significant threshold for $p < 0.05$. Student's t-values above $+2$ or below -2
353 indicate respectively an enrichment or an impoverishment of cell wall components in low
354 compared to high R:FR. **(C)** Student's t-values for wavelengths assigned to cell wall
355 components were used to build the heatmap with negative and positive t-values respectively
356 represented by a range of colors from blue to orange.

357 **Figure 3. Low R:FR triggers changes in the expression of cell wall-related genes. (A)**
358 Number of cell wall-related genes identified as expressed in seedling and regulated by low
359 R:FR in hypocotyl, cotyledon or both. From cell wall-selected genes and RNA sequencing
360 data (Kohnen *et al.* 2016), Venn diagrams highlight cell wall-related genes expressed in
361 seedling and that are regulated by low R:FR in hypocotyl, cotyledon or both. For each,
362 number of up and down-regulated genes are shown along the kinetic of low R:FR treatment.

363 Percentages of the low R:FR-regulated genes were determined according to the total of cell
364 wall-related genes expressed in seedling. **(B)** Number of cell wall-related genes expressed in
365 seedling and regulated by low R:FR classified according to their putative function in cell wall
366 synthesis, remodeling and signaling as well as their related networks for synthesis and
367 remodeling. Percentages were determined according to the total of cell wall-related genes
368 classified for each condition (values between brackets). Network 1: cellulose and
369 hemicelluloses ; Network 2: pectins ; Network 3: structural proteins ; CW: Cell Wall.

370 **Figure 4. Analysis of mutants impaired in cell wall metabolism reveals importance of**
371 **CGR2 and CGR3 in the regulation of the hypocotyl growth and the elastic properties**
372 **under low R:FR. (A)** Length of the hypocotyls in response to low R:FR treatment. Seedlings
373 were grown for 4 days in high R:FR and then for 3 additional days in low R:FR. Data of
374 growth induced by low R:FR during the 3 days were normalized against the wild-type and
375 expressed in log₂FC. Significant differences ($p < 0.05^*$, $p < 0.001^{***}$) were determined
376 according to Student's t-test. **(B)** Length of the hypocotyls in response to high and low R:FR
377 treatments in Col-0 and *cgr2cgr3*. Seedlings were grown for 4 days in high R:FR before being
378 transferred under low R:FR (blue bars) or kept in high R:FR (yellow bars) for 3 additional
379 days. The bars show means in mm \pm confidence intervals measured at 4 (4d), 5 (4d+1d) and 7
380 (4d+3d) days. Significant differences (indicated with letters) were determined according to
381 one-way Anova followed by a multiple comparisons with Tukey's test. **(C)** Elastic properties
382 of hypocotyl assessed under high and low R:FR treatment for Col-0 and *cgr2cgr3*.
383 Hypocotyls were frozen and thawed then subjected to cyclic loading at 5 mN of force and the
384 strain compared to the data obtained for the wild-type seedlings in Figure 2. The average
385 magnitude of strain incurred by seedlings grown in a high R:FR or low R:FR light regime
386 after one (4d+1d) and three days (4d+3d) is shown. The bars show means in % \pm SD ($n > 10$
387 independent seedlings for Col-0 and $n > 5$ independent seedlings for *cgr2cgr3*, at least five
388 oscillations were made per seedling). Pairwise comparisons were made between the mutant
389 and the wild-type using Welch t-test brackets indicated statistical tests that were made with
390 significance $p < 0.1^*$, $p < 0.05^{**}$ and $p < 0.01^{***}$.

391 **Figure 5. Changes of cell wall properties that occur in response to low R:FR are reduced**
392 **in *cgr2cgr3***

393 **(A,B)** Cell wall properties in the middle part of the hypocotyl under high and low R:FR
394 treatments for Col-0 and *cgr2cgr3*. Cell wall chemical bounds were analyzed by Fourier-
395 Transformed InfraRed (FTIR) microspectroscopy. For each hypocotyl, 6 spectra were
396 collected in the middle part, avoiding the central cylinder, for at least 5 independent
397 hypocotyls per condition. Baseline correction and data normalization were made for the
398 absorbances between 1810 and 830 cm^{-1} (corresponding to the cell wall fingerprint, see
399 **Supplemental Figure S6**). Pairwise comparison between high and low R:FR was made after
400 1 and 3 days treatments for Col-0 and *cgr2cgr3* and significant differences were identified
401 using Student's t-test for each wavelength. **(A)** All Student's t-values were plotted against
402 wavelengths with horizontal lines referring to significant threshold for $p < 0.05$ for Col-0 (left
403 panel) and *cgr2cgr3* (right panel). Student's t-values above +2 or below -2 indicate
404 respectively an enrichment or an impoverishment of cell wall components in low compared to

405 high R:FR. **(B)** Student's t-values for wavelengths assigned to cell wall components were
406 used to build the heatmap with negative and positive t-values respectively represented by a
407 range of colors from blue to orange.

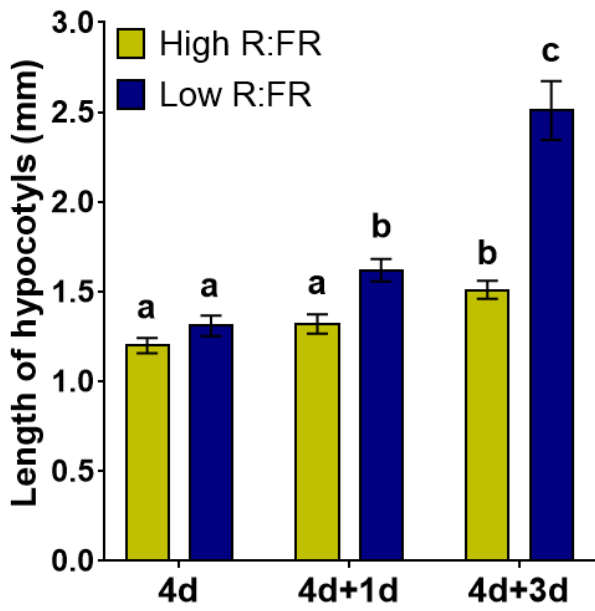
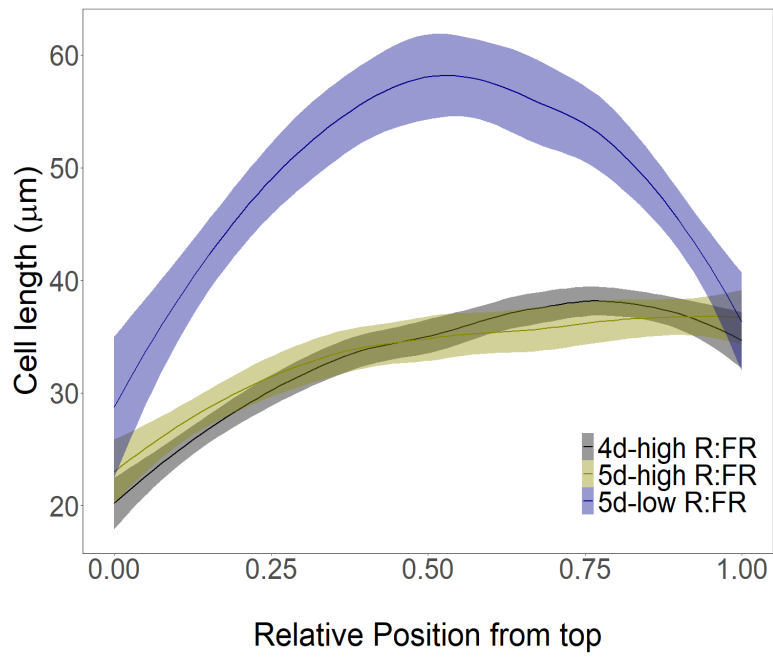
408 **Literature cited**

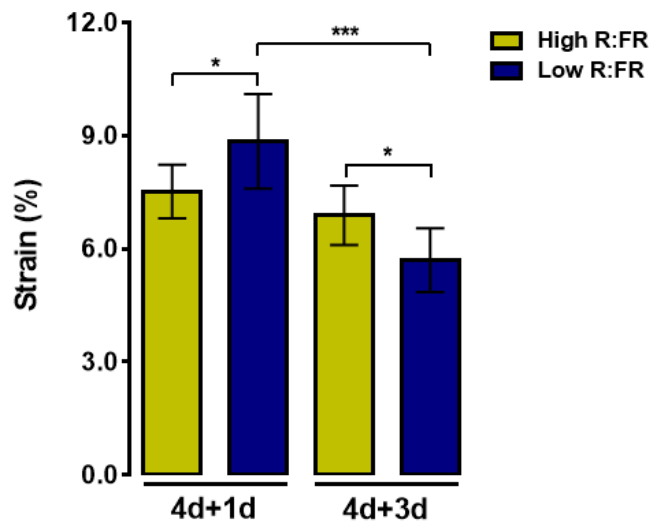
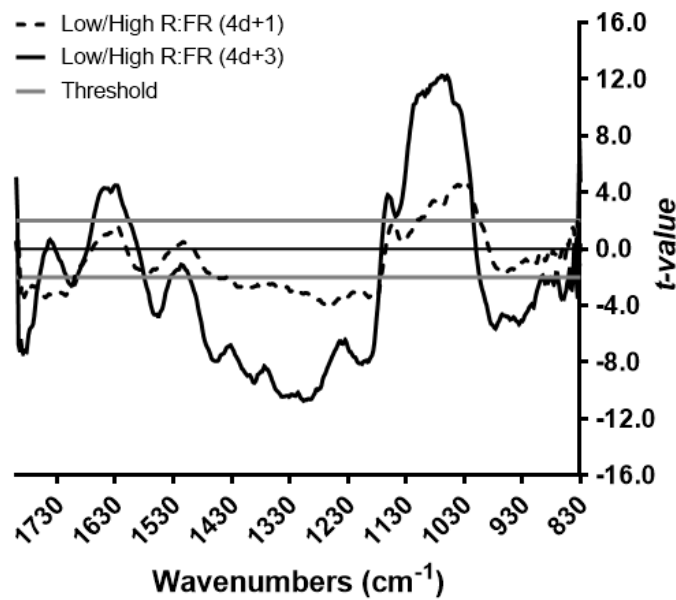
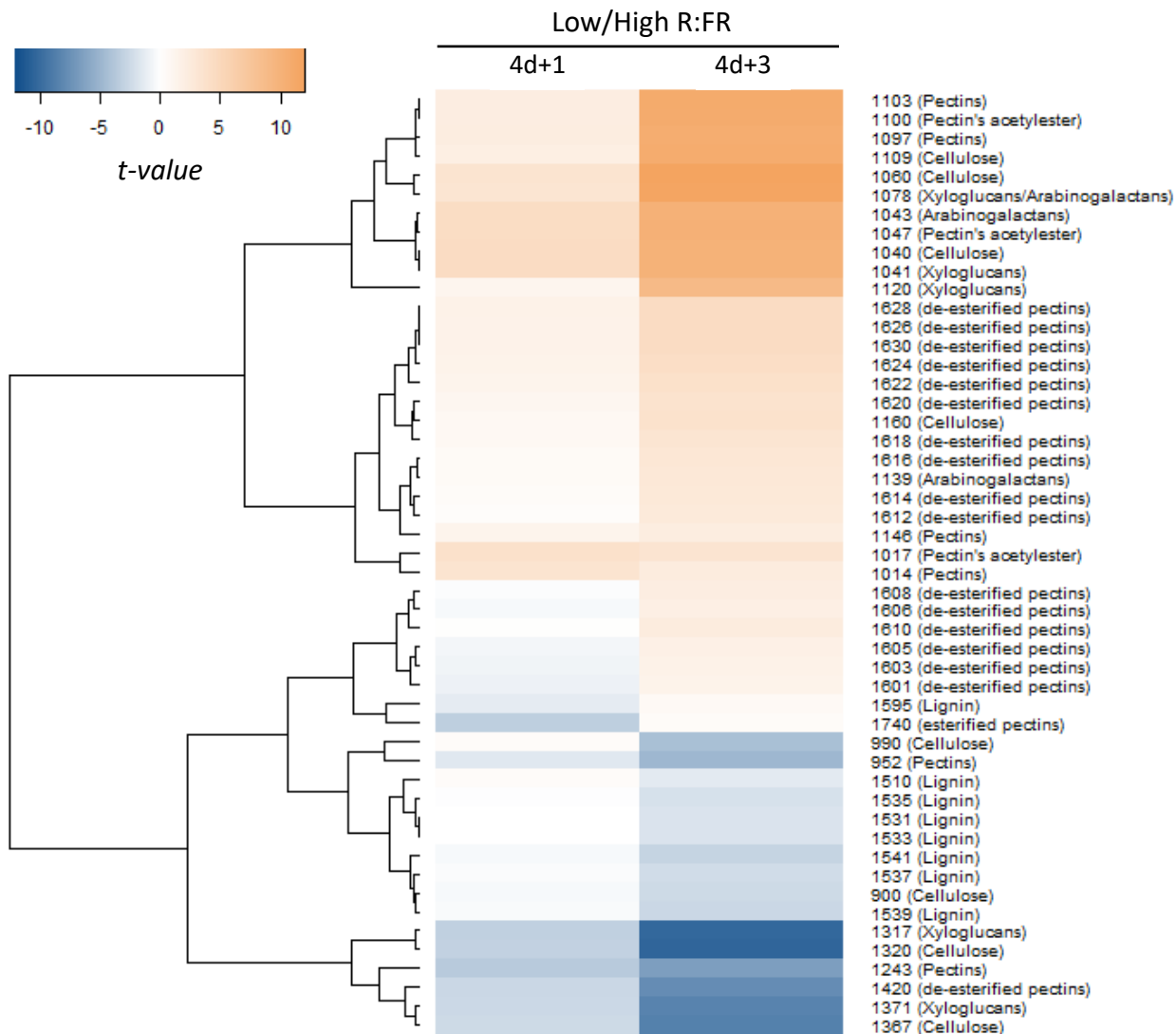
- 409 **Alonso-simón A, García-angulo P, Mérida H, Encina A, Álvarez JM, Acebes JL** (2011)
410 The use of FTIR spectroscopy to monitor modifications in plant cell wall architecture
411 caused by cellulose biosynthesis inhibitors The use of FTIR spectroscopy to monitor
412 modifications in plant cell wall architecture caused by cellulose biosynthesis inhibi. *Plant*
413 *Signal Behav* **6**: 1104–1110
- 414 **Atmodjo MA, Hao Z, Mohnen D** (2013) Evolving Views of Pectin Biosynthesis. *Annu Rev*
415 *Plant Biol* **64**: 747–779
- 416 **Ballaré CL, Pierik R** (2017) The shade-avoidance syndrome: Multiple signals and ecological
417 consequences. *Plant Cell Environ* **40**: 2530–2543
- 418 **Bashline L, Lei L, Li S, Gu Y** (2014) Cell wall, cytoskeleton, and cell expansion in higher
419 plants. *Mol Plant* **7**: 586–600
- 420 **Bouton S** (2002) QUASIMODO1 Encodes a Putative Membrane-Bound Glycosyltransferase
421 Required for Normal Pectin Synthesis and Cell Adhesion in Arabidopsis. *Plant Cell*
422 *Online* **14**: 2577–2590
- 423 **Braybrook SA, Peaucelle A** (2013) Mechano-Chemical Aspects of Organ Formation in
424 *Arabidopsis thaliana*: The Relationship between Auxin and Pectin. *PLoS One*. doi:
425 10.1371/journal.pone.0057813
- 426 **Coen E, Cosgrove DJ** (2023) The mechanics of plant morphogenesis. *Science* **379**: eade8055
- 427 **Cosgrove DJ** (2005) Growth of the plant cell wall. *Nat Rev Mol Cell Biol* **6**: 850–861
- 428 **Fiorucci AS, Fankhauser C** (2017) Plant Strategies for Enhancing Access to Sunlight. *Curr*
429 *Biol* **27**: R931–R940
- 430 **Galvão VC, Fankhauser C** (2015) Sensing the light environment in plants: Photoreceptors
431 and early signaling steps. *Curr Opin Neurobiol* **34**: 46–53
- 432 **Gommers CMM, Visser EJW, Onge KRS, Voesenek LACJ, Pierik R** (2013) Shade
433 tolerance: When growing tall is not an option. *Trends Plant Sci* **18**: 65–71
- 434 **Guénin S, Mareck A, Rayon C, Lamour R, Assoumou Ndong Y, Domon JM, Sénéchal F,**
435 **Fournet F, Jamet E, Canut H, et al** (2011) Identification of pectin methylesterase 3 as
436 a basic pectin methylesterase isoform involved in adventitious rooting in *Arabidopsis*
437 *thaliana*. *New Phytol* **192**: 114–126
- 438 **Hijazi M, Velasquez SM, Jamet E, Estevez JM, Albenne C** (2014) An update on post-
439 translational modifications of hydroxyproline-rich glycoproteins: toward a model
440 highlighting their contribution to plant cell wall architecture. *Front Plant Sci* **5**: 1–10
- 441 **Ince YÇ, Krahmer J, Fiorucci AS, Trevisan M, Galvão VC, Wigger L, Pradervand S,**
442 **Fouillen L, Van Delft P, Genva M, et al** (2022) A combination of plasma membrane
443 sterol biosynthesis and autophagy is required for shade-induced hypocotyl elongation.
444 *Nat Commun*. doi: 10.1038/s41467-022-33384-9
- 445 **Kakuráková M, Capek P, Sasinkova V, Wellner N, Ebringerova A, Kac M** (2000) FT-IR
446 study of plant cell wall model compounds : pectic polysaccharides and hemicelluloses.

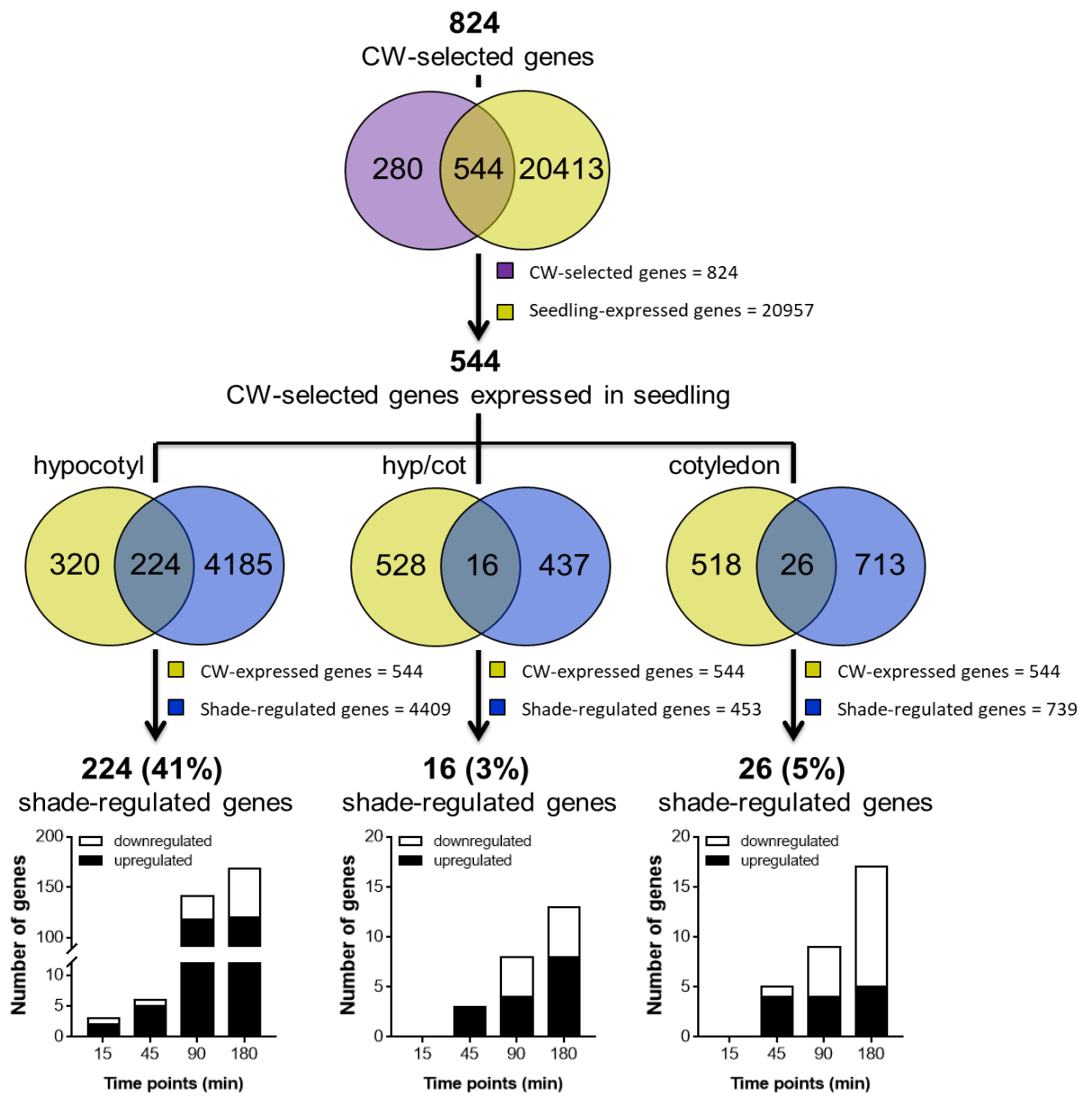
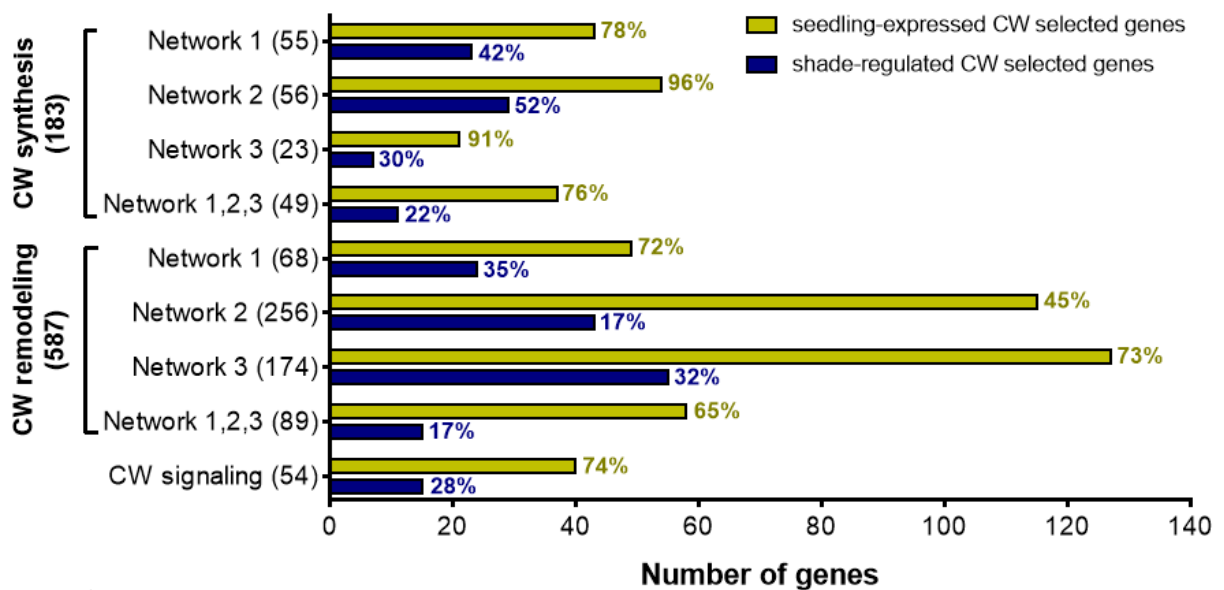
- 447 Carbohydr Polym **43**: 195–203
- 448 **Kim S-J, Held MA, Zemelis S, Wilkerson C, Brandizzi F** (2015) CGR2 and CGR3 have
449 critical overlapping roles in pectin methylesterification and plant growth in *Arabidopsis*
450 *thaliana*. *Plant J* **82**: 208–20
- 451 **Kohnen M V., Schmid-Siegert E, Trevisan M, Petrolati LA, Sénéchal F, Müller-Moulé**
452 **P, Maloof J, Xenarios I, Fankhauser C** (2016) Neighbor detection induces organ-
453 specific transcriptomes, revealing patterns underlying hypocotyl-specific growth. *Plant*
454 *Cell* **28**: 2889–2904
- 455 **Largo-Gosens A, Hernández-Altamirano M, García-Calvo L, Alonso-Simón A,**
456 **Álvarez J, Acebes JL** (2014) Fourier transform mid infrared spectroscopy applications
457 for monitoring the structural plasticity of plant cell walls. *Front Plant Sci* **5**: 1–15
- 458 **Legris M, Ince YÇ, Fankhauser C** (2019) Molecular mechanisms underlying phytochrome-
459 controlled morphogenesis in plants. *Nat Commun* **10**: 1–15
- 460 **Mouille G, Ralet MC, Cavelier C, Eland C, Effroy D, Hématy K, McCartney L, Truong**
461 **HN, Gaudon V, Thibault JF, et al** (2007) Homogalacturonan synthesis in *Arabidopsis*
462 *thaliana* requires a Golgi-localized protein with a putative methyltransferase domain.
463 *Plant J* **50**: 605–614
- 464 **Mouille G, Robin S, Lecomte M, Pagant S, Höfte H** (2003) Classification and identification
465 of *Arabidopsis* cell wall mutants using Fourier-Transform InfraRed (FT-IR)
466 microspectroscopy. *Plant J* **35**: 393–404
- 467 **Nguema-Ona E, Vicré-Gibouin M, Gotté M, Plancot B, Lerouge P, Bardor M,**
468 **Driouich A** (2014) Cell wall O-glycoproteins and N-glycoproteins: aspects of
469 biosynthesis and function. *Front Plant Sci* **5**: 1–12
- 470 **Pauly M, Keegstra K** (2016) Biosynthesis of the Plant Cell Wall Matrix Polysaccharide
471 Xyloglucan. *Annu Rev Plant Biol* **67**: 235–259
- 472 **Peaucelle A, Braybrook SA, Le Guillou L, Bron E, Kuhlemeier C, Höfte H** (2011) Pectin-
473 induced changes in cell wall mechanics underlie organ initiation in *Arabidopsis*. *Curr*
474 *Biol* **21**: 1720–1726
- 475 **Peaucelle A, Louvet R, Johansen JN, Höfte H, Laufs P, Pelloux J, Mouille G** (2008)
476 *Arabidopsis* Phyllotaxis Is Controlled by the Methyl-Esterification Status of Cell-Wall
477 Pectins. *Curr Biol* **18**: 1943–1948
- 478 **Peaucelle A, Wightman R, Höfte H** (2015) The Control of Growth Symmetry Breaking in
479 the *Arabidopsis* Hypocotyl. *Curr Biol* **25**: 1746–1752
- 480 **Pedmale U V., Huang SSC, Zander M, Cole BJ, Hetzel J, Ljung K, Reis PAB, Sridevi P,**
481 **Nito K, Nery JR, et al** (2016) Cryptochromes Interact Directly with PIFs to Control
482 Plant Growth in Limiting Blue Light. *Cell* **164**: 233–245
- 483 **Pelletier S, Van Orden J, Wolf S, Vissenberg K, Delacourt J, Ndong YA, Pelloux J,**
484 **Bischoff V, Urbain A, Mouille G, et al** (2010) A role for pectin de-methylesterification
485 in a developmentally regulated growth acceleration in dark-grown *Arabidopsis*
486 hypocotyls. *New Phytol* **188**: 726–739

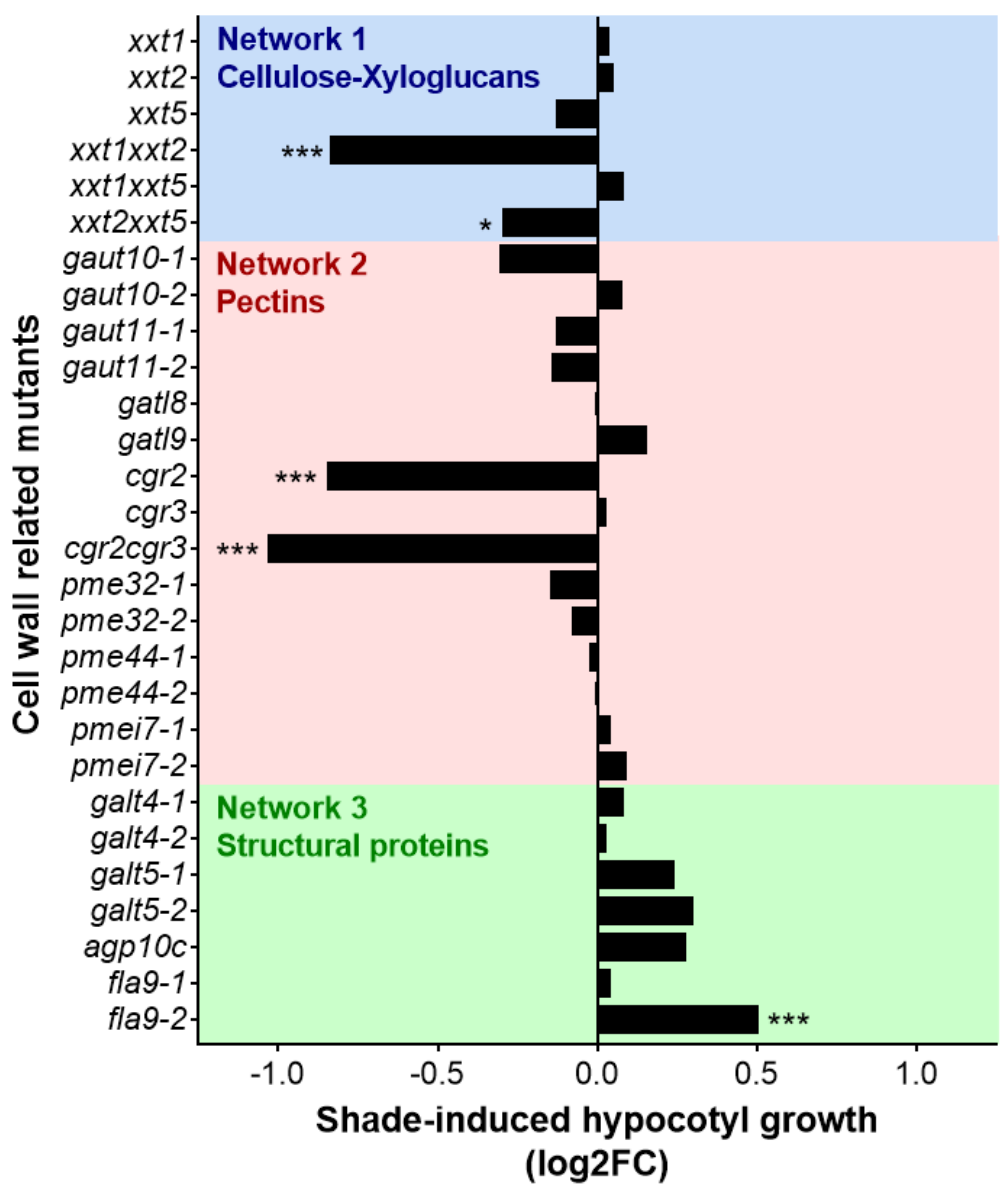
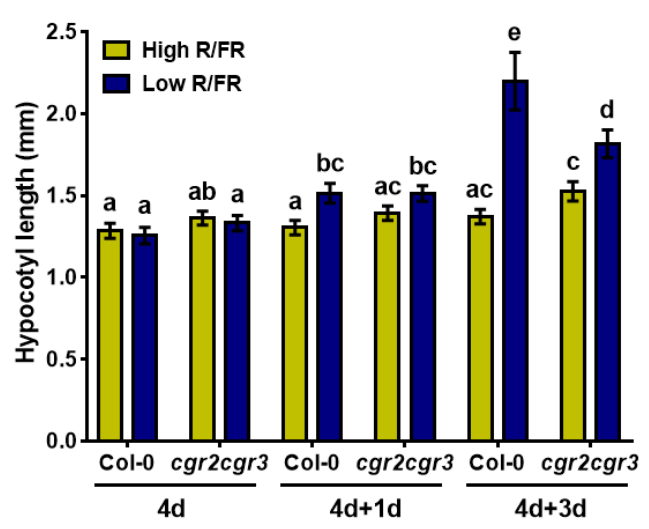
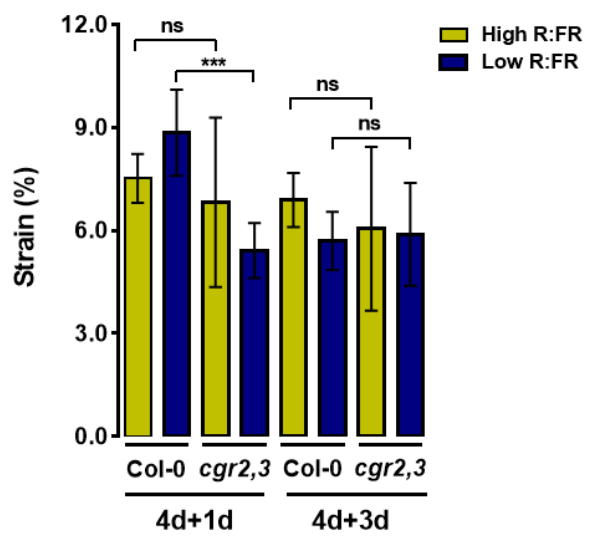
- 487 **Pierik R, De Wit M** (2014) Shade avoidance: Phytochrome signalling and other aboveground
488 neighbour detection cues. *J Exp Bot* **65**: 2815–2824
- 489 **Procko C, Crenshaw CM, Ljung K, Noel JP, Chory J** (2014) Cotyledon-generated auxin is
490 required for shade-induced hypocotyl growth in brassica rapa. *Plant Physiol* **165**: 1285–
491 1301
- 492 **Pucciariello O, Legris M, Costigliolo C, José M, Esteban C, Dezar C, Vazquez M,**
493 **Yanovsky MJ, Finlayson SA, Prat S, et al** (2018) Rewiring of auxin signaling under
494 persistent shade. *Proc Natl Acad Sci* 2–7
- 495 **de Reuille PB, Routier-Kierzkowska AL, Kierzkowski D, Bassel GW, Schüpbach T,**
496 **Tauriello G, Bajpai N, Strauss S, Weber A, Kiss A, et al** (2015) MorphoGraphX: A
497 platform for quantifying morphogenesis in 4D. *Elife* **4**: 1–20
- 498 **Robinson S, Huflejt M, Barbier de Reuille P, Braybrook SA, Schorderet M, Reinhardt**
499 **D, Kuhlemeier C** (2017) An automated confocal micro-extensometer enables in vivo
500 quantification of mechanical properties with cellular resolution. *Plant Cell*
501 tpc.00753.2017
- 502 **Rui Y, Xiao C, Yi H, Kandemir B, Wang JZ, Puri VM, Anderson CT** (2017)
503 POLYGALACTURONASE INVOLVED IN EXPANSION3 Functions in Seedling
504 Development, Rosette Growth, and Stomatal Dynamics in *Arabidopsis thaliana*. *Plant*
505 *Cell* **29**: 2413–2432
- 506 **Sasidharan R, Chinnappa CC, Staal M, Elzenga JTM, Yokoyama R, Nishitani K,**
507 **Voesenek LACJ, Pierik R** (2010) Light Quality-Mediated Petiole Elongation in
508 *Arabidopsis* during Shade Avoidance Involves Cell Wall Modification by Xyloglucan
509 Endotransglucosylase/Hydrolases. *Plant Physiol* **154**: 978–990
- 510 **Sasidharan R, Chinnappa CC, Voesenek LACJ, Pierik R** (2008) The Regulation of Cell
511 Wall Extensibility during Shade Avoidance: A Study Using Two Contrasting Ecotypes
512 of *Stellaria longipes*. *Plant Physiol* **148**: 1557–1569
- 513 **Sasidharan R, Pierik R** (2010) Cell wall modification involving XTHs controls
514 phytochrome-mediated petiole elongation in *Arabidopsis thaliana*. *Plant Signal Behav* **5**:
515 1491–1492
- 516 **Sénéchal F, Graff L, Surcouf O, Marcelo P, Rayon C, Bouton S, Mareck A, Mouille G,**
517 **Stintzi A, Höfte H, et al** (2014a) *Arabidopsis* PECTIN METHYLESTERASE17 is co-
518 expressed with and processed by SBT3.5, a subtilisin-like serine protease. *Ann Bot* **114**:
519 1161–1175
- 520 **Sénéchal F, Wattier C, Rustérucci C, Pelloux J** (2014b) Homogalacturonan-modifying
521 enzymes: Structure, expression, and roles in plants. *J Exp Bot* **65**: 5125–5160
- 522 **Showalter AM, Basu D** (2016) Extensin and Arabinogalactan-Protein Biosynthesis:
523 Glycosyltransferases, Research Challenges, and Biosensors. *Front Plant Sci* **7**: 1–9
- 524 **Szymanska-Chargot M, Zdunek A** (2013) Use of FT-IR Spectra and PCA to the Bulk
525 Characterization of Cell Wall Residues of Fruits and Vegetables Along a Fraction
526 Process. *Food Biophys* **8**: 29–42
- 527 **Wang H, Guo Y, Lv F, Zhu H, Wu S, Jiang Y, Li F, Zhou B, Guo W, Zhang T** (2010)

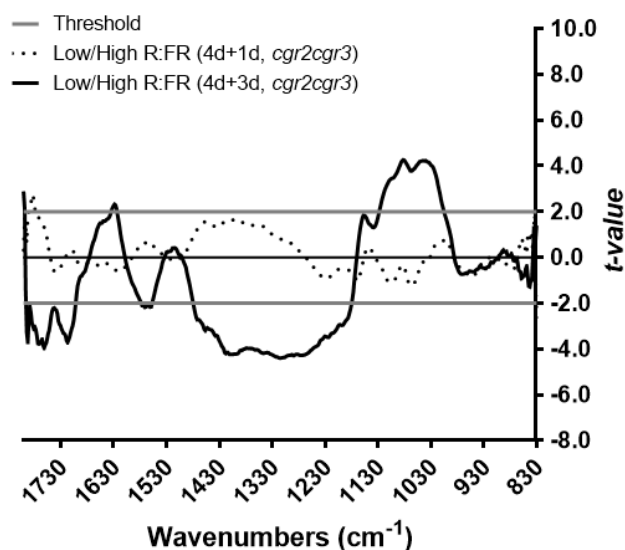
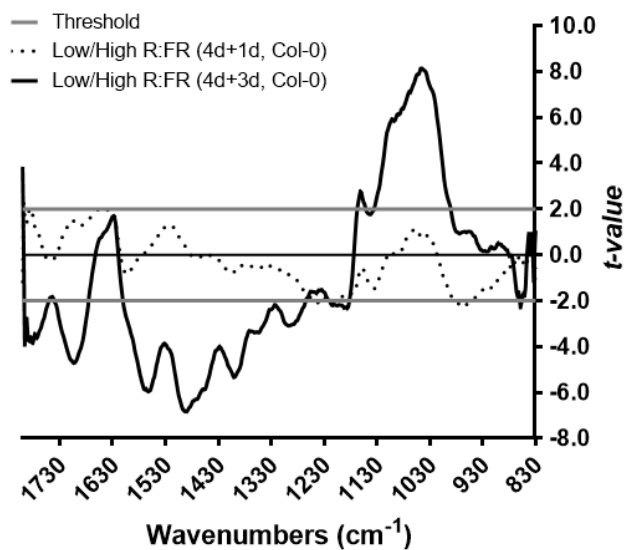
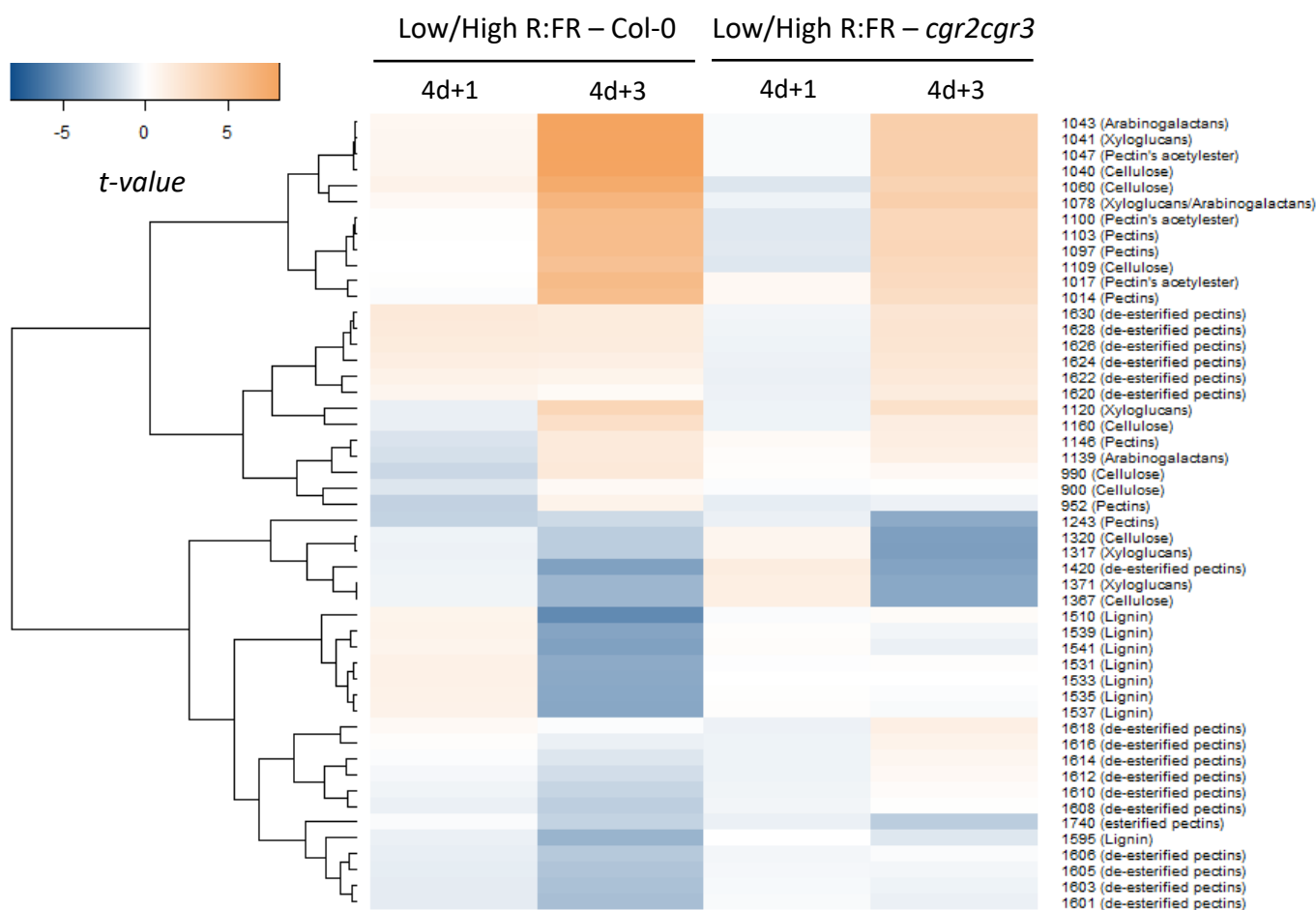
- 528 The essential role of GhPEL gene, encoding a pectate lyase, in cell wall loosening by
529 depolymerization of the de-esterified pectin during fiber elongation in cotton. *Plant Mol*
530 *Biol* **72**: 397–406
- 531 **Wang X, Wilson L, Cosgrove DJ** (2020) Pectin methylesterase selectively softens the onion
532 epidermal wall yet reduces acid-induced creep. *J Exp Bot* **71**: 2629–2640
- 533 **Wilson RH, Smith AC, Kac M, Saunders PK, Wellner N, Waldron KW** (2000) The
534 Mechanical Properties and Molecular Dynamics of Plant Cell Wall Polysaccharides
535 Studied by Fourier-Transform Infrared Spectroscopy 1. *Plant Physiol* **124**: 397–405
- 536 **de Wit M, Galvão VC, Fankhauser C** (2016) Light-Mediated Hormonal Regulation of Plant
537 Growth and Development. *Annu Rev Plant Biol* **67**: 513–537
- 538 **de Wit M, Lorrain S, Fankhauser C** (2014) Auxin-mediated plant architectural changes in
539 response to shade and high temperature. *Physiol Plant* **151**: 13–24
- 540 **Wolf S, Hématy K, Höfte H** (2012a) Growth Control and Cell Wall Signaling in Plants.
541 *Annu Rev Plant Biol* **63**: 381–407
- 542 **Wolf S, Mravec J, Greiner S, Mouille G, Höfte H** (2012b) Plant cell wall homeostasis is
543 mediated by brassinosteroid feedback signaling. *Curr Biol* **22**: 1732–1737
- 544 **Xiao C, Somerville C, Anderson CT** (2014) POLYGALACTURONASE INVOLVED IN
545 EXPANSION1 Functions in Cell Elongation and Flower Development in Arabidopsis.
546 *Plant Cell* **26**: 1018–1035
- 547

A**B****Figure 1**

A**B****C****Figure 2**

A**B****Figure 3**

A**B****C****Figure 4**

A**B****Figure 5**

Parsed Citations

Alonso-simón A, García-angulo P, Mérida H, Encina A, Álvarez JM, Acebes JL (2011) The use of FTIR spectroscopy to monitor modifications in plant cell wall architecture caused by cellulose biosynthesis inhibitors The use of FTIR spectroscopy to monitor modifications in plant cell wall architecture caused by cellulose biosynthesis inhibi. *Plant Signal Behav* 6: 1104–1110

Google Scholar: [Author Only](#) [Title Only](#) [Author and Title](#)

Atmodjo MA, Hao Z, Mohnen D (2013) Evolving Views of Pectin Biosynthesis. *Annu Rev Plant Biol* 64: 747–779

Google Scholar: [Author Only](#) [Title Only](#) [Author and Title](#)

Ballaré CL, Pierik R (2017) The shade-avoidance syndrome: Multiple signals and ecological consequences. *Plant Cell Environ* 40: 2530–2543

Google Scholar: [Author Only](#) [Title Only](#) [Author and Title](#)

Bashline L, Lei L, Li S, Gu Y (2014) Cell wall, cytoskeleton, and cell expansion in higher plants. *Mol Plant* 7: 586–600

Google Scholar: [Author Only](#) [Title Only](#) [Author and Title](#)

Bouton S (2002) QUASIMODO1 Encodes a Putative Membrane-Bound Glycosyltransferase Required for Normal Pectin Synthesis and Cell Adhesion in Arabidopsis. *Plant Cell Online* 14: 2577–2590

Google Scholar: [Author Only](#) [Title Only](#) [Author and Title](#)

Braybrook SA, Peaucelle A (2013) Mechano-Chemical Aspects of Organ Formation in Arabidopsis thaliana: The Relationship between Auxin and Pectin. *PLoS One*. doi: 10.1371/journal.pone.0057813

Google Scholar: [Author Only](#) [Title Only](#) [Author and Title](#)

Coen E, Cosgrove DJ (2023) The mechanics of plant morphogenesis. *Science* 379: eade8055

Google Scholar: [Author Only](#) [Title Only](#) [Author and Title](#)

Cosgrove DJ (2005) Growth of the plant cell wall. *Nat Rev Mol Cell Biol* 6: 850–861

Google Scholar: [Author Only](#) [Title Only](#) [Author and Title](#)

Fiorucci AS, Fankhauser C (2017) Plant Strategies for Enhancing Access to Sunlight. *Curr Biol* 27: R931–R940

Google Scholar: [Author Only](#) [Title Only](#) [Author and Title](#)

Galvão VC, Fankhauser C (2015) Sensing the light environment in plants: Photoreceptors and early signaling steps. *Curr Opin Neurobiol* 34: 46–53

Google Scholar: [Author Only](#) [Title Only](#) [Author and Title](#)

Gommers CMM, Visser EJW, Onge KRS, Voeselek LACJ, Pierik R (2013) Shade tolerance: When growing tall is not an option. *Trends Plant Sci* 18: 65–71

Google Scholar: [Author Only](#) [Title Only](#) [Author and Title](#)

Guénin S, Mareck A, Rayon C, Lamour R, Assoumou Ndong Y, Domon JM, Sénéchal F, Fournet F, Jamet E, Canut H, et al (2011) Identification of pectin methylesterase 3 as a basic pectin methylesterase isoform involved in adventitious rooting in Arabidopsis thaliana. *New Phytol* 192: 114–126

Google Scholar: [Author Only](#) [Title Only](#) [Author and Title](#)

Hijazi M, Velasquez SM, Jamet E, Estevez JM, Albenne C (2014) An update on post-translational modifications of hydroxyproline-rich glycoproteins: toward a model highlighting their contribution to plant cell wall architecture. *Front Plant Sci* 5: 1–10

Google Scholar: [Author Only](#) [Title Only](#) [Author and Title](#)

Ince YÇ, Krahmer J, Fiorucci AS, Trevisan M, Galvão VC, Wigger L, Pradervand S, Fouillen L, Van Delft P, Genva M, et al (2022) A combination of plasma membrane sterol biosynthesis and autophagy is required for shade-induced hypocotyl elongation. *Nat Commun*. doi: 10.1038/s41467-022-33384-9

Google Scholar: [Author Only](#) [Title Only](#) [Author and Title](#)

Kakuráková M, Capek P, Sasinkova V, Wellner N, Ebringerova A, Kac M (2000) FT-IR study of plant cell wall model compounds: pectic polysaccharides and hemicelluloses. *Carbohydr Polym* 43: 195–203

Google Scholar: [Author Only](#) [Title Only](#) [Author and Title](#)

Kim S-J, Held MA, Zemelis S, Wilkerson C, Brandizzi F (2015) CGR2 and CGR3 have critical overlapping roles in pectin methylesterification and plant growth in Arabidopsis thaliana. *Plant J* 82: 208–20

Google Scholar: [Author Only](#) [Title Only](#) [Author and Title](#)

Kohnen M V., Schmid-Siegert E, Trevisan M, Petrolati LA, Sénéchal F, Müller-Moulé P, Maloof J, Xenarios I, Fankhauser C (2016) Neighbor detection induces organ-specific transcriptomes, revealing patterns underlying hypocotyl-specific growth. *Plant Cell* 28: 2889–2904

Google Scholar: [Author Only](#) [Title Only](#) [Author and Title](#)

Largo-Gosens A, Hernández-Altamirano M, García-Calvo L, Alonso-Simón A, Álvarez J, Acebes JL (2014) Fourier transform mid

infrared spectroscopy applications for monitoring the structural plasticity of plant cell walls. *Front Plant Sci* 5: 1–15

Google Scholar: [Author Only](#) [Title Only](#) [Author and Title](#)

Legris M, Ince YÇ, Fankhauser C (2019) Molecular mechanisms underlying phytochrome-controlled morphogenesis in plants. *Nat Commun* 10: 1–15

Google Scholar: [Author Only](#) [Title Only](#) [Author and Title](#)

Mouille G, Ralet MC, Cavelier C, Eland C, Effroy D, Hématy K, McCartney L, Truong HN, Gaudon V, Thibault JF, et al (2007) Homogalacturonan synthesis in *Arabidopsis thaliana* requires a Golgi-localized protein with a putative methyltransferase domain. *Plant J* 50: 605–614

Google Scholar: [Author Only](#) [Title Only](#) [Author and Title](#)

Mouille G, Robin S, Lecomte M, Pagant S, Höfte H (2003) Classification and identification of *Arabidopsis* cell wall mutants using Fourier-Transform InfraRed (FT-IR) microspectroscopy. *Plant J* 35: 393–404

Google Scholar: [Author Only](#) [Title Only](#) [Author and Title](#)

Nguema-Ona E, VitrÃ©-Gibouin M, GottÃ© M, Plancot B, Lerouge P, Bardor M, Driouch A (2014) Cell wall O-glycoproteins and N-glycoproteins: aspects of biosynthesis and function. *Front Plant Sci* 5: 1–12

Google Scholar: [Author Only](#) [Title Only](#) [Author and Title](#)

Pauly M, Keegstra K (2016) Biosynthesis of the Plant Cell Wall Matrix Polysaccharide Xyloglucan. *Annu Rev Plant Biol* 67: 235–259

Google Scholar: [Author Only](#) [Title Only](#) [Author and Title](#)

Peaucelle A, Braybrook SA, Le Guillou L, Bron E, Kuhlemeier C, Höfte H (2011) Pectin-induced changes in cell wall mechanics underlie organ initiation in *Arabidopsis*. *Curr Biol* 21: 1720–1726

Google Scholar: [Author Only](#) [Title Only](#) [Author and Title](#)

Peaucelle A, Louvet R, Johansen JN, Höfte H, Laufs P, Pelloux J, Mouille G (2008) *Arabidopsis* Phyllotaxis Is Controlled by the Methyl-Esterification Status of Cell-Wall Pectins. *Curr Biol* 18: 1943–1948

Google Scholar: [Author Only](#) [Title Only](#) [Author and Title](#)

Peaucelle A, Wightman R, Höfte H (2015) The Control of Growth Symmetry Breaking in the *Arabidopsis* Hypocotyl. *Curr Biol* 25: 1746–1752

Google Scholar: [Author Only](#) [Title Only](#) [Author and Title](#)

Pedmale U V., Huang SSC, Zander M, Cole BJ, Hetzel J, Ljung K, Reis PAB, Sridevi P, Nito K, Nery JR, et al (2016) Cryptochromes Interact Directly with PIFs to Control Plant Growth in Limiting Blue Light. *Cell* 164: 233–245

Google Scholar: [Author Only](#) [Title Only](#) [Author and Title](#)

Pelletier S, Van Orden J, Wolf S, Vissenberg K, Delacourt J, Ndong YA, Pelloux J, Bischoff V, Urbain A, Mouille G, et al (2010) A role for pectin de-methylesterification in a developmentally regulated growth acceleration in dark-grown *Arabidopsis* hypocotyls. *New Phytol* 188: 726–739

Google Scholar: [Author Only](#) [Title Only](#) [Author and Title](#)

Pierik R, De Wit M (2014) Shade avoidance: Phytochrome signalling and other aboveground neighbour detection cues. *J Exp Bot* 65: 2815–2824

Google Scholar: [Author Only](#) [Title Only](#) [Author and Title](#)

Procko C, Crenshaw CM, Ljung K, Noel JP, Chory J (2014) Cotyledon-generated auxin is required for shade-induced hypocotyl growth in *brassica rapa*. *Plant Physiol* 165: 1285–1301

Google Scholar: [Author Only](#) [Title Only](#) [Author and Title](#)

Pucciariello O, Legris M, Costigliolo C, José M, Esteban C, Dezar C, Vazquez M, Yanovsky MJ, Finlayson SA, Prat S, et al (2018) Rewiring of auxin signaling under persistent shade. *Proc Natl Acad Sci* 2–7

Google Scholar: [Author Only](#) [Title Only](#) [Author and Title](#)

de Reuille PB, Routier-Kierzkowska AL, Kierzkowski D, Bassel GW, Schüpbach T, Tauriello G, Bajpai N, Strauss S, Weber A, Kiss A, et al (2015) MorphoGraphX: A platform for quantifying morphogenesis in 4D. *Elife* 4: 1–20

Google Scholar: [Author Only](#) [Title Only](#) [Author and Title](#)

Robinson S, Huflejt M, Barbier de Reuille P, Braybrook SA, Schorderet M, Reinhardt D, Kuhlemeier C (2017) An automated confocal micro-extensometer enables in vivo quantification of mechanical properties with cellular resolution. *Plant Cell tpc.00753.2017*

Google Scholar: [Author Only](#) [Title Only](#) [Author and Title](#)

Rui Y, Xiao C, Yi H, Kandemir B, Wang JZ, Puri VM, Anderson CT (2017) POLYGALACTURONASE INVOLVED IN EXPANSION3 Functions in Seedling Development, Rosette Growth, and Stomatal Dynamics in *Arabidopsis thaliana*. *Plant Cell* 29: 2413–2432

Google Scholar: [Author Only](#) [Title Only](#) [Author and Title](#)

Sasidharan R, Chinnappa CC, Staal M, Elzenga JTM, Yokoyama R, Nishitani K, Voesenek LACJ, Pierik R (2010) Light Quality-

Mediated Petiole Elongation in Arabidopsis during Shade Avoidance Involves Cell Wall Modification by Xyloglucan Endotransglucosylase/Hydrolases. Plant Physiol 154: 978–990

Google Scholar: [Author Only](#) [Title Only](#) [Author and Title](#)

Sasidharan R, Chinnappa CC, Voesenek LACJ, Pierik R (2008) The Regulation of Cell Wall Extensibility during Shade Avoidance: A Study Using Two Contrasting Ecotypes of *Stellaria longipes*. Plant Physiol 148: 1557–1569

Google Scholar: [Author Only](#) [Title Only](#) [Author and Title](#)

Sasidharan R, Pierik R (2010) Cell wall modification involving XTHs controls phytochrome-mediated petiole elongation in *Arabidopsis thaliana*. Plant Signal Behav 5: 1491–1492

Google Scholar: [Author Only](#) [Title Only](#) [Author and Title](#)

Sénéchal F, Graff L, Surcouf O, Marcelo P, Rayon C, Bouton S, Mareck A, Mouille G, Stintzi A, Höfte H, et al (2014a) Arabidopsis PECTIN METHYLESTERASE17 is co-expressed with and processed by SBT3.5, a subtilisin-like serine protease. Ann Bot 114: 1161–1175

Google Scholar: [Author Only](#) [Title Only](#) [Author and Title](#)

Sénéchal F, Wattier C, Rustérucci C, Pelloux J (2014b) Homogalacturonan-modifying enzymes: Structure, expression, and roles in plants. J Exp Bot 65: 5125–5160

Google Scholar: [Author Only](#) [Title Only](#) [Author and Title](#)

Showalter AM, Basu D (2016) Extensin and Arabinogalactan-Protein Biosynthesis: Glycosyltransferases, Research Challenges, and Biosensors. Front Plant Sci 7: 1–9

Google Scholar: [Author Only](#) [Title Only](#) [Author and Title](#)

Szymanska-Chargot M, Zdunek A (2013) Use of FT-IR Spectra and PCA to the Bulk Characterization of Cell Wall Residues of Fruits and Vegetables Along a Fraction Process. Food Biophys 8: 29–42

Google Scholar: [Author Only](#) [Title Only](#) [Author and Title](#)

Wang H, Guo Y, Lv F, Zhu H, Wu S, Jiang Y, Li F, Zhou B, Guo W, Zhang T (2010) The essential role of GhPEL gene, encoding a pectate lyase, in cell wall loosening by depolymerization of the de-esterified pectin during fiber elongation in cotton. Plant Mol Biol 72: 397–406

Google Scholar: [Author Only](#) [Title Only](#) [Author and Title](#)

Wang X, Wilson L, Cosgrove DJ (2020) Pectin methylesterase selectively softens the onion epidermal wall yet reduces acid-induced creep. J Exp Bot 71: 2629–2640

Google Scholar: [Author Only](#) [Title Only](#) [Author and Title](#)

Wilson RH, Smith AC, Kac M, Saunders PK, Wellner N, Waldron KW (2000) The Mechanical Properties and Molecular Dynamics of Plant Cell Wall Polysaccharides Studied by Fourier-Transform Infrared Spectroscopy 1. Plant Physiol 124: 397–405

Google Scholar: [Author Only](#) [Title Only](#) [Author and Title](#)

de Wit M, Galvão VC, Fankhauser C (2016) Light-Mediated Hormonal Regulation of Plant Growth and Development. Annu Rev Plant Biol 67: 513–537

Google Scholar: [Author Only](#) [Title Only](#) [Author and Title](#)

de Wit M, Lorrain S, Fankhauser C (2014) Auxin-mediated plant architectural changes in response to shade and high temperature. Physiol Plant 151: 13–24

Google Scholar: [Author Only](#) [Title Only](#) [Author and Title](#)

Wolf S, Hématy K, Höfte H (2012a) Growth Control and Cell Wall Signaling in Plants. Annu Rev Plant Biol 63: 381–407

Google Scholar: [Author Only](#) [Title Only](#) [Author and Title](#)

Wolf S, Mravec J, Greiner S, Mouille G, Höfte H (2012b) Plant cell wall homeostasis is mediated by brassinosteroid feedback signaling. Curr Biol 22: 1732–1737

Google Scholar: [Author Only](#) [Title Only](#) [Author and Title](#)

Xiao C, Somerville C, Anderson CT (2014) POLYGALACTURONASE INVOLVED IN EXPANSION1 Functions in Cell Elongation and Flower Development in Arabidopsis. Plant Cell 26: 1018–1035

Google Scholar: [Author Only](#) [Title Only](#) [Author and Title](#)